International Journal of Mass Spectrometry 298 (2010) 64–71

Contents lists available at ScienceDirect

International Journal of Mass Spectrometry

journal homepage: www.elsevier.com/locate/ijms

Improved analysis of explosives samples with electrospray ionization-high resolution ion mobility spectrometry (ESI-HRIMS)

Christopher K. Hilton, Clinton A. Krueger, Anthony J. Midey, Mark Osgood, Jianglin Wu, Ching Wu*

Excellims Corporation, 20 Main Street, Acton, MA 01720, USA

ARTICLE INFO

Article history:
Received 23 May 2009
Received in revised form 3 June 2010
Accepted 13 August 2010
Available online 9 September 2010

Keywords:
Ion mobility
Electrospray
Explosive
High resolution

ABSTRACT

A novel high resolution ion mobility spectrometer (HRIMS) equipped with an electrospray ionization (ESI) source was used to analyze trace levels of several energetic materials. The ESI-HRIMS system allowed rapid analysis of explosive samples that were difficult to detect using conventional IMS systems while providing resolving powers, R, greater than 60 and good sensitivity toward the troublesome homemade explosives (HME). This research demonstrated analysis of trace levels of explosives in both positive and negative ion modes, including thermally labile explosives such as TATP and PETN that are detected as their intact molecular ions. Ion mobility spectra and reduced mobility values (K_o) of common explosives were reported in good agreement with previously published values. The high performance IMS system provided a rapid, effective analytical tool that was a suitable upgrade for current explosive sample screening and routine analysis applications.

1. Introduction

Ion mobility spectrometers (IMSs) have become common tools for detecting trace levels of explosives in a variety of homeland security and force protection detection scenarios [1–5]. IMS-based detection systems are among the most widely used chemical detection methods at airports, high security buildings, customs, and other security check points. IMS characterizes substances based on their velocity as gas phase ions moving in an electric field. Swarms of these ions will achieve a constant velocity, v, as they move through a voltage gradient at ambient pressure proportional to the electric field, E, in the IMS, where v is related to the proportionality constant known as the mobility, K, for a given substance (see Eq. (1)). Differences in the mobilities give different drift velocities, thus different drift times, separating the various chemical components. The mobility is fundamentally related to a combination of the ion's size/shape, charge, q, reduced mass, μ, for collisions with the neutral inert drift gas and their interaction potential, which consequently affects their collision cross-section, Ω_d [1,6]. Compared to other spectrometric chemical analysis technologies, e.g., mass spectrometry, IMS is a relatively low resolution technique. However, IMS does benefit from very high sensitivity, good scalability, low power consumption, and ambient pressure operation. Many currently deployed IMS systems utilize thermal desorption of a sample from a swab in conjunction with a radioactive ^{63}Ni beta ionization source [1–4]. While this combination is effective for detecting particular energetic materials, thermally labile materials suffer from degradation in the desorber and are not detected effectively [3,4]. Although a radioactive ionization source provides reliable field operational performance, the combination of thermal desorption followed by ionization by a radioactive source is not a viable approach for all analytes of interest.

Electrospray ionization-ion mobility spectrometry (ESI-IMS) was first demonstrated by Shumate and Hill [7]. Numerous researchers have since demonstrated the potential of using ESI-IMS for the analysis of a variety of semi-volatile and non-volatile compounds, including environmental contaminants [8–10], illicit drugs [11–17], pharmaceuticals [18–22], chemical warfare agents [23–25], explosives [26–29] and biological molecules [30–33]. The bulk of the research has been performed on custom-built instruments in academic or government research labs. Until recently, commercially available IMS instruments with an ESI source have been unavailable. One newer commercial instrument utilizes ESI with traveling-wave ion mobility spectrometry (TW-IMS) [34,35]. In this method, a series of symmetric potential waves continuously pass through a drift tube to propel ions with a velocity, v, determined by their mobility, K, shown in Eq. (1) below for a typical drift time IMS with field, E [1,6,35]:

$$K = \frac{v}{E} \propto \frac{q}{\mu^{1/2}\Omega_d} \quad (1)$$

Current applications of TW-IMS include the analysis of complex biological and macrocyclic structures [31,36–39].

* Corresponding author. Tel.: +1 978 264 1980; fax: +1 978 264 1981.
E-mail address: ching.wu@excellims.com (C. Wu).

1387-3806/$ – see front matter © 2010 Elsevier B.V. All rights reserved.
doi:10.1016/j.ijms.2010.08.011

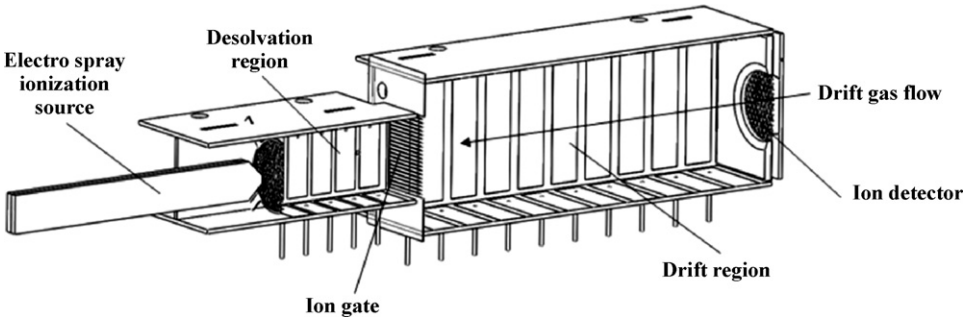

Fig. 1. Excellims GA-2100 High Resolution Ion Mobility Spectrometer (HRIMS) fitted with an electrospray ionization (ESI) source.

Moreover, a traditional drift time IMS with an ESI source is also now available commercially. The previous difficulties in producing an instrument of this type with ESI has been partially attributed to the complexity of introducing liquid phase samples into a high temperature drift tube under ambient pressure conditions, then managing the voltage requirements associated with the source and IMS drift tube [40,41]. In this work, results are presented using the first commercially available drift time ESI-IMS system with high resolution drift tube to provide better analysis of explosive samples in a rapid fashion. A variety of dissolved military/commercial explosive materials have been screened; specifically, Primasheet, Detasheet, PETN, Semtex A, Semtex H, HMX, C4, and TNT. In addition, homemade explosives (HME) ammonium nitrate (AN), urea nitrate (UN) and triacetone triperoxide (TATP) have been successfully detected with the ESI-HRIMS, which is more amenable to reliable detection of thermally labile analytes like PETN and TATP as intact molecular ions [42,43]. Detection of these threats is limited in current explosives trace detection (ETD) systems employing thermal desorption sample introduction where the compounds decompose at the high temperatures inside the desorber, in contrast to the "softer" ionization via ESI for sample introduction. These ETDs capabilities can be further hindered by the presence of other components in the sample that have similar mobilities as the target, such as other explosives, binder materials or impurities [3,4]. The higher resolution of the HRIMS vs. current ETDs can resolve all of these components into individual peaks and use this additional information to better confirm the identity of the material. In addition, preliminary data are presented that indicate that this high resolution system can generate quantitative or semi-quantitative information about explosives composition for routine explosives sample analysis.

2. Materials and methods

This research was conducted using a commercially available electrospray ionization-high resolution ion mobility spectrometer (ESI-HRIMS) from Excellims Corporation (Acton, MA), as shown in Fig. 1. Analyte ions were generated by ESI from liquid samples continuously infused through a 100 μm ID fused silica capillary tube into the ion source at flow rates between 3 and 8 μl min^{-1} using a Chemyx Fusion 100 syringe pump (Stafford, TX). The electrospray needle was held 4.3 kV DC above the drift potential with a current limitation of 1 μA total current. The ionized droplets underwent desolvation in the desolvation region and were subsequently introduced into the drift tube held at a constant temperature of 150 °C via a pulsed Bradbury–Neilson ion gate with gate pulse widths from 50 to 100 μs. The upper potential of the desolvation region of the IMS was held at 8000 VDC and the gate reference voltage was held at approximately 7000 VDC, producing a drift field of around 645 V cm^{-1} over the 10.85 cm long drift tube. The potentials are negative polarity for negative ions and positive polarity for positive ions. Ions were separated according to the their size/shape, reduced mass, μ, and charge, q, as they moved under the influence of the drift field through the 0.8 l min^{-1} of counter-flowing drift gas in the drift region as discussed below. The mobility spectrum represented a sum over 10 spectra ranging in length from 10 to 25 ms depending on the drift time of the analyte ions, which were then sampled at a Faraday plate detector. Data were acquired using Excellims VisIon^{TM} control and acquisition software and were exported for post-processing to Microsoft Excel. Atmospheric pressure in the laboratory was monitored and recorded for all experiments to properly correct the drift spectra as shown below.

In the drift time ion mobility spectrometer, ions drifted through a counter-flowing drift gas under the influence of an electric field, E, with a velocity, v, as shown in Eq. (1) above and were separated based on their mobility, K. For a drift tube of length, L, with applied potential, V, the drift field, E, and ion velocity, v, could be expressed as shown in Eqs. (2) and (3), respectively, given below, where t_d was the drift time of the given analyte ion:

$$E = \frac{V}{L} \tag{2}$$

$$v = \frac{L}{t_d} \tag{3}$$

Thus, the mobility could be expressed as a function of these parameters as shown in Eq. (4):

$$E = \frac{L^2}{Vt_d} \tag{4}$$

The mobility measured was relevant only under the given experimental conditions. Therefore, K could be converted to a mobility defined under standard conditions, K_0, known as the reduced mobility, illustrated in Eq. (5), where P was the drift tube operating pressure (in. Hg) and T_d was the temperature of the drift tube in Kelvin:

$$K_0 = K\left(\frac{P}{29.92}\right)\left(\frac{273.15}{T_d}\right) \tag{5}$$

Converting to a reduced mobility allowed for direct comparison to mobilities measured in other drift time IMS experiments [1].

Unless noted, the experiments were performed using high performance liquid chromatography (HPLC) grade solvents, including methanol, water, and acetic acid (Sigma–Aldrich). Urea nitrate (UN) was synthesized using the known reaction of urea (Sigma–Aldrich) and nitric acid (Sigma–Aldrich) [44,45]. The product was rinsed and a known mass of pure UN was then dissolved in methanol to produce the desired stock solution concentration. The remaining energetic materials were provided by the Transportation Safety Laboratory (TSL) as concentrated liquid stock solutions of known concentration that were diluted to suitable concentrations either in pure methanol or in a solvent mixture of 80% methanol and 20% water (v/v), with 0.5% acetic acid by volume added for the positive ion mode experiments. The IMS drift gas was pure nitrogen

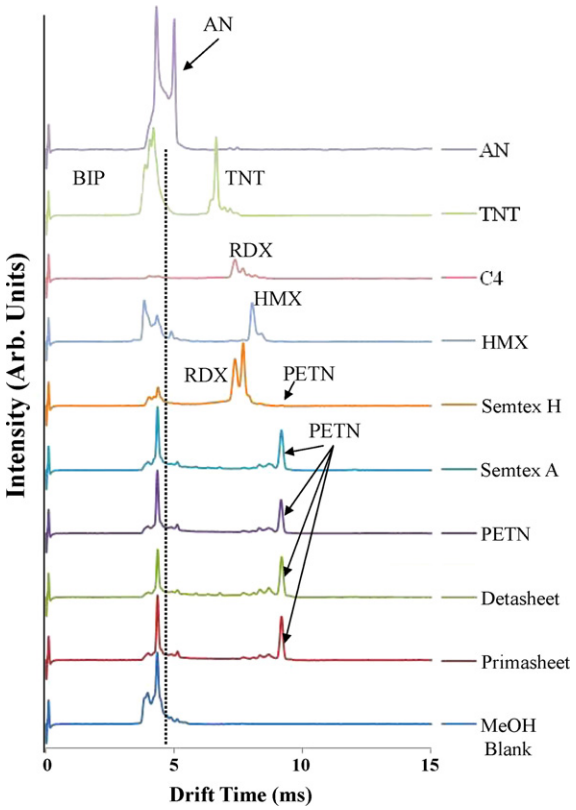

Fig. 2. Electrospray ionization (ESI)-high resolution ion mobility spectra (HRIMS) of several types of explosives measured in negative ion mode in nitrogen drift gas at 150 °C. The ion intensity is plotted against the drift time in ms. The peaks to the left of the dashed line at shorter drift times are the background ion peaks (BIP) and the peaks to the right of the dashed line at longer drift times are the analyte ions labeled accordingly.

(99.999%, AirGas). The chemicals were used as obtained without further purification, except for passing the drift gas through a 13X molecular sieve trap (Fluka) before entering the IMS drift tube to ensure the removal of any water vapor or other contaminants.

3. Results and discussion

Using an instrument with high resolution and high sensitivity, analyte ions that are produced with a lower relative intensity may also be observed and used for verifying the identity of ions in the sample. Fig. 2 shows example high resolution ion mobility spectra measured for nine explosive samples in negative ion mode operation. A liquid infusion flow rate for the electrospray ionization source of 8 μl min^{-1} and a solution concentration of 0.1 μg μl^{-1} (100 ng μl^{-1}) has been used for these experiments to generate spectra with high signal to noise ratio to illustrate the HRIMS capabilities.

The total amount of energetic material introduced to the ionization source for each spectrum in Fig. 2 is approximately 6 ng, reflecting the sum of 30 spectra, each of which is 15 ms in length. The nine explosive compositions studied contain five major energetic compounds; specifically, ammonium nitrate (AN); 2,4,6-trinitrotoluene (TNT); 1,3,5-trinitro-1,3,5-triazacyclohexane (RDX), pentaerythritol tetranitrate (PETN); and 1,3,5,7-tetranitro-1,3,5,7-tetrazocane (HMX). For the composite explosive compounds such as C4 and Semtex, the fraction of the explosive agent present in each composition is summarized in Table 1. All of these explosive compounds can be separated and detected. Differences in the background ion peaks (BIP) for the various explosives in Fig. 2 reflect differences in the ESI conditions caused by analyzing samples prepared from dissolving the actual explosive compound which will have different amounts of other material added during manufacturing. The data for the composite explosive materials and the homemade explosives are further analyzed by class and major explosive compound in the following sections.

Table 1
Explosive compositions by fractional content (%).[a]

Explosive	PETN	RDX	HMX	TNT	TATP	AN
Detasheet	63	–	–	–	–	–
Primasheet	65	–	–	–	–	–
Semtex A	94	6	–	–	–	–
Semtex H	50	50	–	–	–	–
C4	–	>88	<12	–	–	–
PETN	100	–	–	–	–	–
HMX	–	–	<100[b]	–	–	–
TNT	–	–	–	100	–	–
TATP	–	–	–	–	100	–
AN	–	–	–	–	–	100

[a] Explosive compositions are obtained from common literature [59,60], and used for the purpose of gaining general understanding of the IMS data. The actual composition of the dissolved military explosives used in this study was not confirmed using other analytical methods.
[b] Typical HMX production has a yield of about 55–60%, with RDX as an impurity.

3.1. Trinitrotoluene (TNT)

The ESI-HRIMS spectrum for 6 ng of TNT at 150 °C is shown in Fig. 2. TNT is typically detected as a single peak in commercial IMS explosive detectors and is well studied in the literature [1,4,26,28,29]. Similarly, a single strong peak is also observed in the ESI-HRIMS having a reduced mobility of $K_0 = 1.59\ \mathrm{cm^2\ V^{-1}\ s^{-1}}$, which is in good agreement with the literature values using N_2 drift gas [4].

Fig. 3a shows an ion mobility spectrum of TNT under similar operating conditions using an IMS with the same drift tube construction as in the experiments in Fig. 2. However, the spectrum has been obtained using a diluted sample created by dissolving actual explosive material, not a purified reference sample. The trace components such as binder material can vary, resulting in different reactant ion peak distributions for a given sample as seen in Fig. 2, depending on the ability to ionize these unknown components. The resolving power, R, for TNT with drift time t_d is 70 using Eq. (6) below [1], where $\Delta t_{1/2}$ is the width at half maximum of the ion intensity:

$$R = \frac{t_d}{\Delta t_{1/2}} \tag{6}$$

2.3 times the resolving power of a commercial IMS-based explosives detector, where a 4 ng TNT sample analyzed with that system has R around 40, as illustrated in the spectrum shown in Fig. 3b [46]. The improved performance can be attributed to the drift tube construction that provides greater field uniformity for the ions along the drift axis and increased accuracy in the time base from better gate control electronics that provides narrower, more precise gate pulses.

One way to consider IMS is in regards to its separating ability, i.e., using properties of the chemical analytes to differentiate and/or identify the peaks. To facilitate comparison with more traditional chromatographic methods, the resolving power for IMS in Eq. (6) can be recast in terms of a number of theoretical plates, N. This parameter is commonly used for comparing the separating ability of typical chromatographic methods and is defined in Eq. (7) for IMS [47]. Consequently, N for the chromatographic methods can be used to determine a resolving power R for comparison with IMS,

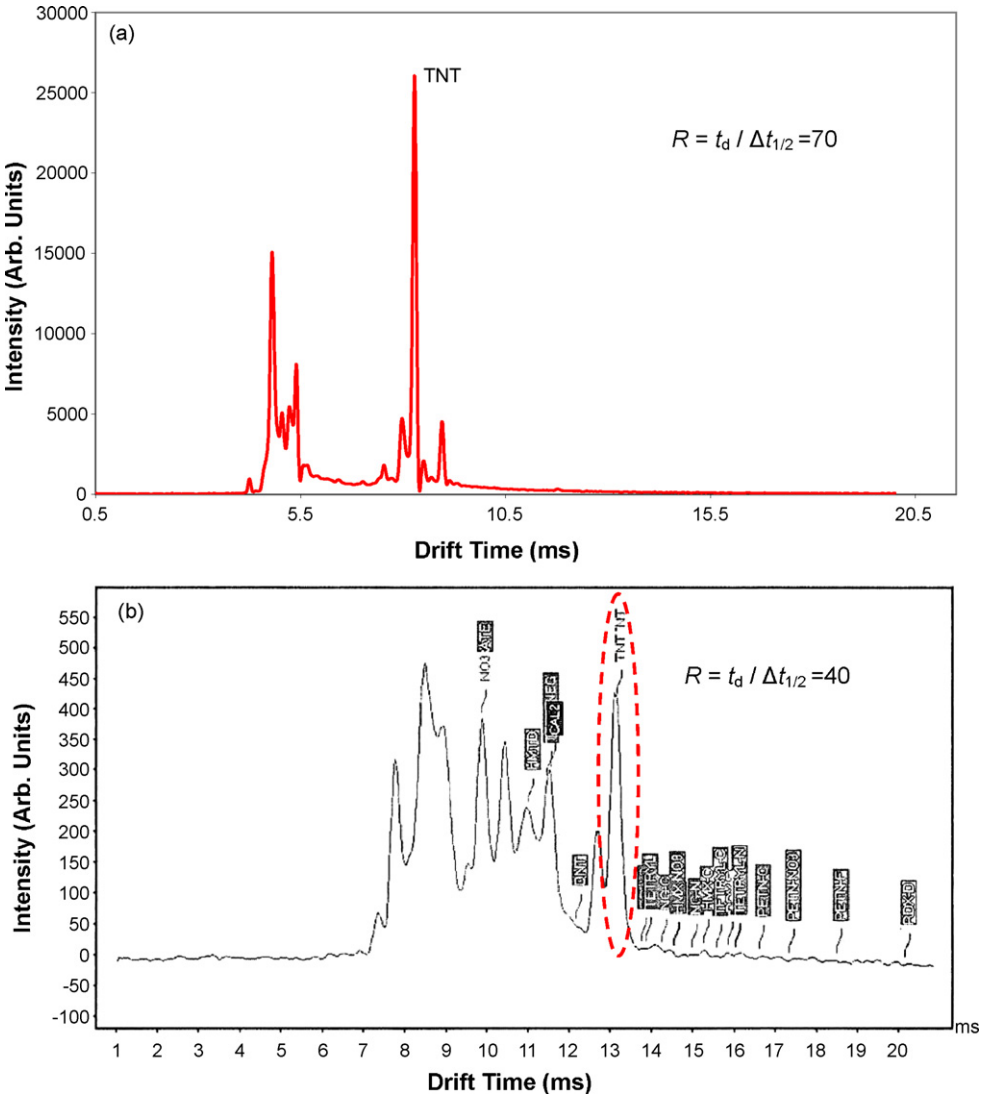

Fig. 3. (a) Ion mobility spectrum of TNT measured using ESI-HRIMS. (b) Ion mobility spectrum of 4 ng of TNT measured by Danylewych-May using a commercial IMS-based explosives detector (ETD). The TNT peak is indicated by the red oval. See Ref. [46]. (For interpretation of the references to color in this figure legend, the reader is referred to the web version of the article.)

strictly on the ability to separate analyte peaks:

$$N = 5.55\left(\frac{t_d}{w_h}\right)^2 \quad (7)$$

When defined in these terms, the standalone ESI-HRIMS has resolving power approaching that commonly achieved with HPLC [47]. The high resolving power is directly related to the peak capacity of this analytical method, which, in turn, is of fundamental importance for field-analysis of explosives where the explosives, their precursors, interferences and other related compounds all need to be identified.

3.2. PETN-based rubberized sheet explosives

Fig. 4 shows ion mobility spectra of PETN and four PETN-based explosives, where the sample was prepared by dissolving the explosive in various solvents in concentrations of 100 ng μl^{-1}. The spectrum for the blank methanol solvent can be seen in Fig. 2 for comparison. The nominal proportions of PETN in the composite explosives are: Detasheet 63%, Primasheet 65%, Semtex A 94%, Semtex H 50%, and PETN standard 100% by weight. The main peak demonstrates resolving power of around 63. The response of the IMS system shown in Fig. 4 does not reflect the ratios of the theoretical composition, but instead similar peak heights are observed in the spectra. In fact, Semtex H shows a very weak mobility peak for PETN. As will be discussed in the next section for RDX explosives, charge competition will hinder the response to the explosive having the relatively lower charge affinity, such as PETN. Also, other components will be present in small amounts because the analytes are created from samples of real explosives that include other components in the formula of the plastic explosives. Higher concentration solutions have been used to demonstrate the instrument's capabilities. As such, the concentrations employed for illustrative purposes approach the top of the linear response range, where the system response plateaus. However, typical analyses aim to detect samples with low concentrations, well within the linear range.

Furthermore, three additional peaks between 5.5 and 7 ms have also been detected in the spectra for Detasheet and Semtex A that have similar drift times. As seen in Table 1, Semtex A and Detasheet have the same major explosive component; however, the other chemical ingredients in the composite differ, possibly indicative of similar fragmentation of the ions formed. However, if these are

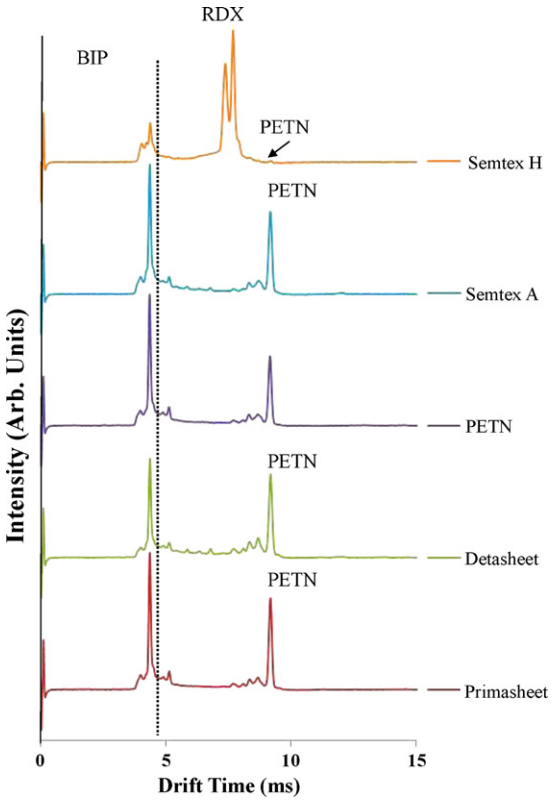

Fig. 4. Electrospray ionization (ESI)-high resolution ion mobility spectra (HRIMS) of PETN-based explosives measured in negative ion mode in nitrogen drift gas at 150 °C. The ion intensity is plotted against the drift time in ms. The peaks to the left of the dashed line at shorter drift times are the background ion peaks (BIP) and the peaks to the right of the dashed line at longer drift times are the analyte ions labeled accordingly.

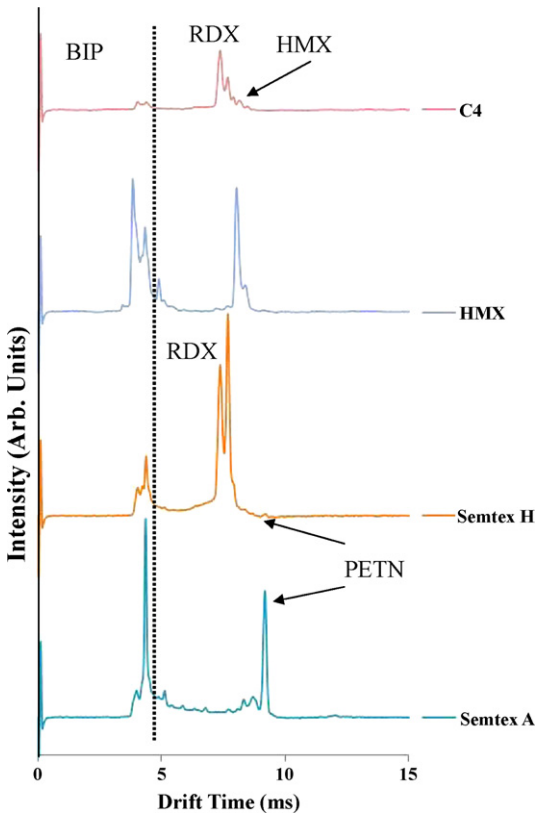

Fig. 5. Electrospray ionization (ESI)-high resolution ion mobility spectra (HRIMS) of RDX-based explosives measured in negative ion mode in nitrogen drift gas at 150 °C. The ion intensity is plotted against the drift time in ms. The peaks to the left of the dashed line at shorter drift times are the background ion peaks (BIP) and the peaks to the right of the dashed line at longer drift times are the analyte ions labeled accordingly.

PETN dissociation product ions, similar peaks should be present in the other PETN composites. Alternatively, these minor peaks may reflect contributions from the other chemical components such as binders and plasticizers found in the composite [42,49], again because the actual explosive composite has been dissolved to prepare the stock solutions of known concentration. For example, both Semtex and Detasheet can be produced using tributyl citrate plasticizer. Thus, the peaks may represent ions produced from these common ingredients or similar degradation products of them [59,60].

All of the PETN-based explosives have a peak in their spectra at a similar drift time of ~9.1 ms. Under our instrumental conditions, this drift time corresponds to a reduced mobility value of $K_o = 1.19\ cm^2\ V^{-1}\ s^{-1}$, which is in good agreement with published values ranging from 1.1 to 1.2 $cm^2\ V^{-1}\ s^{-1}$ where the primary molecular structure is largely intact in the ion detected [1,4,29]. In other commercial IMS-based explosive detection systems, PETN-based explosives are commonly detected as NO_3^- fragment ions because of the use of a thermal desorber that leads to decomposition of the molecule [3,4]. However, by using an electrospray ionization source and a drift tube at 150 °C, the majority of the PETN molecules are not subjected to thermal decomposition. This advantage of ESI and nano-ESI systems is well established and has been exploited for ionizing other types of thermally labile compounds [48]. Nevertheless, for the field of trace detection of explosives, having the ability to detect the intact PETN molecular ion in the ion mobility spectrum of the ESI-HRIMS system enhances the detection selectivity compared to the existing ETDs that employ the desorber sample introduction systems.

3.3. RDX-based explosives

Fig. 5 shows ion mobility spectra for RDX-based explosives. The 100 ng μl^{-1} samples studied have been prepared by diluting stock solutions originally made by dissolving real military explosives to a known concentration. As seen in Table 1, the compositions of these plastic explosives are: C-4: 83% RDX; Semtex A: 94% PETN with 6% RDX; and Semtex H: 50% PETN with 50% RDX. As seen in Fig. 5, the C-4 sample generated both RDX and HMX peaks with a ratio of the peak heights at about 8:1. RDX manufactured using the Bachmann process usually contains about 8–12% HMX as an acceptable byproduct [49,60]. The observed ratio, while not an exact match, is close to the actual theoretical composition, in part, due to the similarities in the molecular structures of RDX and HMX that result in similar charge affinities, thus similar electrospray ionization efficiencies. RDX has two main peaks with reduced mobilities of $K_0 = 1.48$ and 1.42 $cm^2\ V^{-1}\ s^{-1}$ that are in good agreement with literature values [1,4,26,29]. Similar to the PETN-based explosives, these values are indicative of ions where the RDX molecular structure is intact, likely resulting from adduct formation [1,4,26,29]. The HMX sample produces two peaks corresponding to reduced mobilities of $K_o = 1.35$ and 1.30 $cm^2\ V^{-1}\ s^{-1}$. These reduced mobility values are in decent agreement with the literature values measured in air at 250 °C of $K_o = 1.30$ and $K_o = 1.25\ cm^2\ V^{-1}\ s^{-1}$ [4,26].

On the other hand, the intensity ratios of the RDX to PETN peaks in both Figs. 4 and 5 do not match the theoretical compositions for Semtex A and Semtex H in Table 1. This phenomenon could be caused by charge competition between PETN and RDX in the ionization source where the RDX ionizes more readily. As discussed previously, the samples analyzed have been obtained by prepar-

ing stock solutions of the detonatable material, including binders and other possible remnants of their manufacture method. Selective ionization based on differences in the charge affinities of the analytes such as proton affinity and ionization potential has been exploited in IMS to improve detection abilities [1]; however, charge competition can also be detrimental to the sensitivity of explosives detection [50] and are a potential issue with ESI sources [15]. However, both peaks are present at the expected mobility values and Semtex H produces a strong RDX peak. The PETN peak is present, but it remains disproportionately lower in intensity, which may cause difficulty in discriminating between RDX and Semtex.

3.4. Home made explosives (HME)

3.4.1. Ammonium nitrate (AN)

Ammonium nitrate (AN) is among the threats of major concern because it is readily available in large quantities at a low cost per pound for use as fertilizer, but it is especially useful for vehicle-borne improvised explosive devices (VBIEDs). AN is classified as an oxidizer, and when mixed with a fuel (e.g., diesel) it produces a powerful HME referred to as ammonium nitrate-fuel oil (ANFO) [3,59]. Detection of AN using conventional trace detection systems based on thermal desorption followed by ion mobility analysis commonly suffers from poor sensitivity and selectivity. The poor sensitivity is caused by thermal decomposition and in some devices by poor transportation efficiency through a membrane inlet, while the poor selectivity is caused by interference from numerous non-explosive components that overlap with AN fragment ion drift times in an IMS [4].

Fig. 6a depicts the ion mobility spectrum for AN in negative ion mode at 150 °C. With the ESI-HRIMS, the AN is well ionized and easily detected. The high resolution of the HRIMS allows good separation of AN ions. Recently obtained preliminary HRIMS-MS data using Excellims RA4100 ESI-IMS-QMS [51], where the ESI-IMS subsystem is operated under identical conditions as described in experimental section, are shown in Fig. 6b. The two main peaks below 5 ms drift time are NO_3^- and $NO_3^-(HNO_3)$, while the smaller peaks at longer drift time (inset) correspond to larger clusters with $NO_3^-(AN)_3$. Zhao and Yinon have shown in a previous mass spectrometry (MS) study of AN using ESI-MS at a similar electrospray

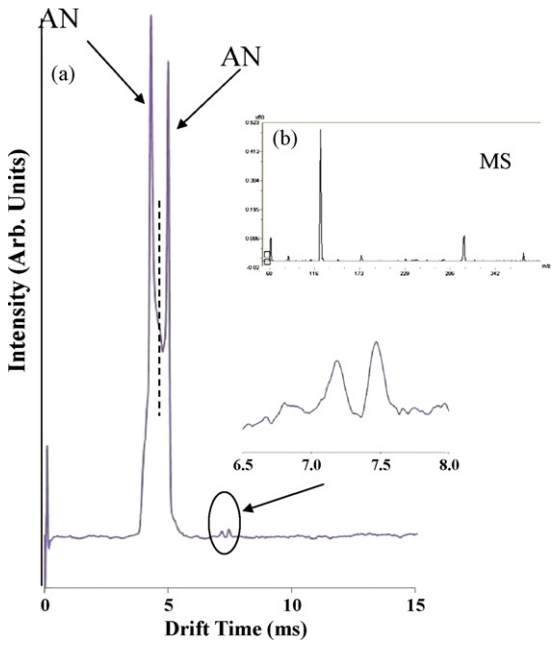

Fig. 6. (a) Electrospray ionization (ESI)-high resolution ion mobility spectra (HRIMS) of ammonium nitrate (AN) measured in negative ion mode in nitrogen drift gas at 150 °C. The ion intensity is plotted against the drift time in ms. The analyte ions are labeled accordingly. (b) Inset graph showing a recently obtained mass spectrum (MS) taken with a new HRIMS-MS instrument.

temperature that the predominate peaks correspond to NO_3^- and the clusters of $[NO_3\cdot(HNO_3)_n]^-$ where $n = 1, 2$. They have also confirmed the identity of the $NO_3^-(AN)_3$ peak through isotopically labeled measurements [52]. Note that the spectrum shown in Fig. 6 demonstrates an ion mobility resolving power of 67.

3.4.2. Triacetone triperoxide (TATP)

Fig. 7a shows positive mode ion mobility spectra from two different TATP samples. TATP is known to be one of the most unstable explosives [53] and is typically detected in positive ion mode [54]. Cooks and co-workers have shown that TATP forms positive ions using DESI sampling doped with alkali chlorides or ammo-

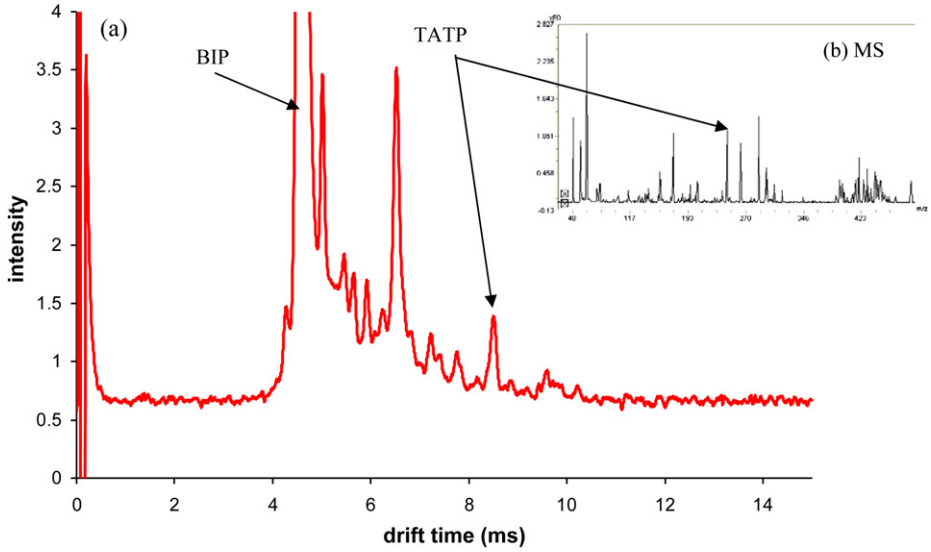

Fig. 7. (a) Electrospray ionization (ESI)-high resolution ion mobility spectra (HRIMS) of triacetone triperoxide (TATP) measured in positive ion mode at 150 °C. The ion intensity is plotted against the drift time in ms. The peaks to the left of the dashed line at shorter drift times are the solvent ion–background ion peaks (BIP) and the peaks at longer drift times are the analyte related ions labeled accordingly. (b) Inset graph showing a recently obtained mass spectrum (MS) taken with a new HRIMS-MS instrument.

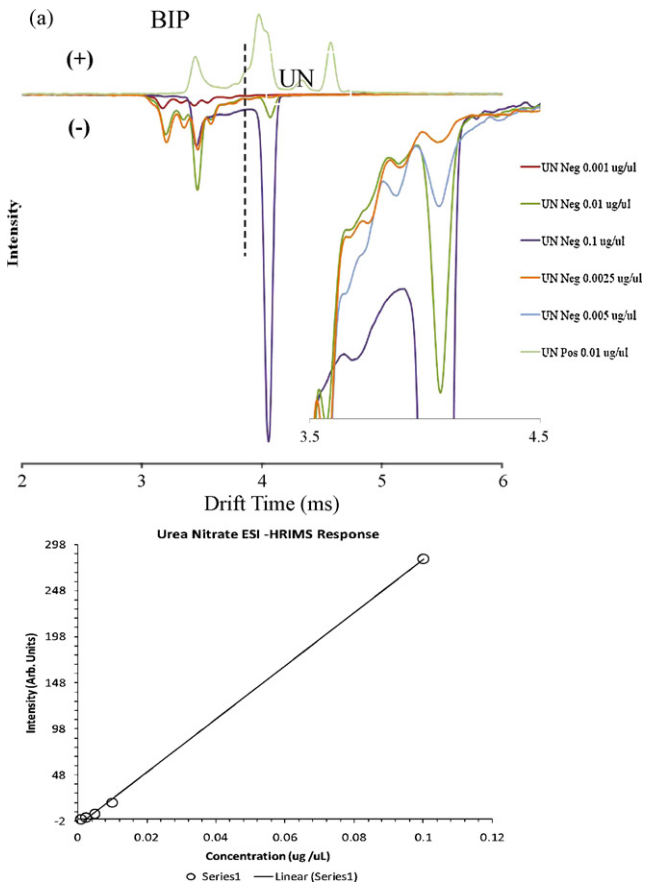

Fig. 8. (a) Electrospray ionization (ESI)-high resolution ion mobility spectra (HRIMS) of urea nitrate (UN) measured in both positive and negative ion mode at 150 °C. The ion intensity is plotted against the drift time in ms. The peaks to the left of the dashed line at shorter drift times are the background ion peaks (BIP) and the peaks to the right of the dashed line at longer drift times are the analyte ions labeled accordingly. The expanded view shows the UN signal intensity as a function of UN sample concentration. (b) Concentration of UN sampled plotted as a function of UN ion intensity.

nium acetate, followed by MS detection. The most significant ions have been mass identified as having $m/z = 223$, 240 and 245 corresponding to $[TATP+H]^+$, $[TATP+NH_4]^+$, and $[TATP+Na]^+$, verified by MS/MS CID experiments [55]. The ammonia-TATP adduct has also been observed in GC-IMS-MS experiments when ammonia dopant is used, along with a dissociation product from acetone cation [56], which forms readily in the gas phase from thermal dissociation of TATP [53]. Denton and co-workers have also observed the $[TATP+H]^+$ in the mass spectrum from an IMS-MS experiment with TATP dissolved in toluene [57]. In the current ESI-HRIMS measurements in positive ion mode, the peak at 8.5 ms is consistent with the $[TATP+Na]^+$ adduct, likely formed from trace amounts of sodium present in the solvents and glass containers [58], confirmed by preliminary HRIMS-MS data where the MS is shown Fig. 7b.

3.4.3. Urea nitrate

Selective, yet sensitive, detection of urea nitrate (UN) poses a new challenge to traditional ion mobility spectrometers equipped with a thermal desorber. Fig. 8a shows the results of using ESI-HRIMS for the analysis of UN in both positive and negative ion mode. The ESI-HRIMS response to UN is extremely sensitive in both positive and negative ion mode. It is worth mentioning that the resolving power of the IMS system is $R > 50$ even when low picograms of analyte are detected. Thus, both high sensitivity and resolution have been achieved. In one aspect, the UN peaks in the positive ion mobility spectra show significantly lower ion mobility (longer drift time) compared to the negative ion spectra, indicating a much larger ion is the signature peak formed in positive ion mode. Similar to the results discussed for the AN samples, the larger cluster ions can provide more target-specific information; thus, higher specificity is achieved with the current instrumental method.

Given the system response to UN, the identification method using ESI-HRIMS may benefit from detecting both positive and negative ions from the same sample. An operational method for the ESI-HRIMS system may be created to acquire data in both polarities during the analysis of the UN samples. Practically, the ESI-HRIMS is currently configured to acquire data in a single polarity which can be switched in seconds; however, these hardware limitations can conceivably be eliminated to allow switching in under a second with the current arrangement.

3.5. Quantitative analysis using the ESI-HRIMS

To assess the ability of the ESI-HRIMS at quantitative measurements, a series of urea nitrate samples at concentrations of 0.0025, 0.005, 0.01, and 0.1 $\mu g\,\mu l^{-1}$ have been introduced into the ion source at an injection rate of 5 $\mu l\,min^{-1}$ and the ion mobility spectra have been measured in negative ion mode. As shown in the expanded view of Fig. 8a, the ESI-HRIMS is very sensitive to UN compared to the current ETDs that struggle detecting it as discussed above. The intensity of the main negative ion peak for UN increases with increasing UN sample concentration as expected. The system demonstrates consistent peak height trends with increasing sample concentration and a dynamic response range of two orders of magnitude. A response curve can be constructed using the data in Fig. 8a that represent a sum over 30 spectra of 15 ms in length at each concentration and is shown in Fig. 8b as the UN ion intensity vs. sample concentration. Good linearity is maintained over two orders of magnitude from 0.0025 $\mu g\,\mu l^{-1}$, which represents 37 pg of UN under the experimental conditions, still with decent signal to noise. Thus, the data indicate that almost a single picogram detection limit should be achievable, making this method valuable for detection of HMEs.

4. Conclusions

In this study, ten military/commercial and homemade explosives (HME) have been analyzed using a commercial electrospray ionization-high resolution ion mobility spectrometer (ESI-HRIMS). The observed ion mobility spectra demonstrate a wealth of identifying information. High resolution IMS ($R = 70$) can provide significantly more detail about sample composition, as extra peaks produced during explosive analysis can be used as an additional indentifying characteristic for more accurate threat identification. The electrospray ionization source has been shown to be particularly effective for polar molecules such as ammonium nitrate (AN) that do not transport or ionize well in conventional ion mobility spectrometry explosive trace detectors (ETDs) that rely on thermal desorption and radioactive ionization sources. In addition, electrospray ionization is also very effective for thermally labile explosives, such as PETN and TATP. Analysis of these compounds using the ESI-HRIMS allows identification of molecular ions, as well as signature product ions that enhance detection confidence as verified by recent IMS-MS data, with preliminary data showing the potential for quantitation. Future studies will be conducted to further explore quantitative measurement of energetic materials in more complex matrices and to maximize the limits of detection. Consequently, an ESI-HRIMS can be used as an effective tool for rapid analysis of common military and homemade explosives.

Acknowledgements

The authors thank Dr. Richard Lareau and his colleagues at Department of Homeland Security (DHS) – Transportation Security Laboratory (TSL) for kindly providing explosive samples.

References

[1] G.A. Eiceman, Z. Karpas, Ion Mobility Spectrometry, 2nd ed., CRC Press, Boca Raton, 2005.
[2] J. Yinon, TrAC Trends Anal. Chem. 21 (2005) 292.
[3] D.S. Moore, Rev. Sci. Instrum. 75 (2004) 2499–2512.
[4] R.G. Ewing, D.A. Atkinson, G.A. Eiceman, G.J. Ewing, Talanta 54 (2001) 515.
[5] F. Li, Z. Xie, H. Schmidt, S. Sielemann, J.I. Baumbach, Spectrochim. Acta B 57 (2002) 1563.
[6] H.E. Revercomb, E.A. Mason, Anal. Chem. 47 (1975) 970.
[7] C.B. Shumate, H.H. Hill Jr., Anal. Chem. 61 (1989) 601.
[8] C. Wu, A.P. Gamerdinger, H.H. Hill Jr., Field Anal. Chem. Technol. 2 (1998) 155–161.
[9] B.H. Clowers, W.E. Steiner, H.M. Dion, L.M. Matz, M. Tam, E.E. Tarver, H.H. Hill, Field Anal. Chem. Technol. 5 (2002) 302.
[10] P. Dwivedi, L.M. Matz, D.A. Atkinson, H.H. Hill Jr., Analyst 129 (2004) 139.
[11] H. Lai, P. Guerra, M. Joshi, J.R. Almirall, J. Sep. Sci. 31 (2008) 402.
[12] M.T. Jafari, Talanta 77 (2009) 1632.
[13] C. Wu, W.F. Siems, H.H. Hill Jr., Anal. Chem. 72 (2000) 396.
[14] W.E. Steiner, B.H. Clowers, K.H. Fuhrer, M. Gonin, L.M. Matz, W.F. Siems, A.J. Schultz, H.H. Hill, Rapid Commun. Mass Spectrom. 15 (2001) 2221.
[15] L.M. Matz, H.H. Hill, Anal. Chem. 74 (2002) 420.
[16] L.M. Matz, H.H. Hill Jr., Anal. Chim. Acta 457 (2002) 235.
[17] L.M. Matz, H.H. Hill Jr., Anal. Chem. 73 (2001) 1664.
[18] P. Dwivedi, C. Wu, L.M. Matz, B.H. Clowers, W.F. Siems, H.H. Hill Jr., Anal. Chem. 78 (2006) 8200.
[19] J.K. Loknauth, N.H. Snow, Anal. Chem. 77 (2005) 5983.
[20] C. Qi, A. Granger, V. Papov, J. McCaffrey, D.L. Norwood, J. Pharm. Biomed. Anal. 51 (2010) 107.
[21] M.A. Strege, Anal. Chem. 81 (2009) 4576.
[22] M.A. Strege, J. Kozerski, N. Juarbe, P. Mahoney, Anal. Chem. 80 (2008) 3040.
[23] W.E. Steiner, B.H. Clowers, L.M. Matz, W.F. Siems, H.H. Hill Jr., Anal. Chem. 74 (2002) 4343.
[24] G.R. Asbury, C. Wu, W.F. Siems, H.H. Hill Jr., Anal. Chim. Acta 404 (2000) 273.
[25] W.E. Steiner, B.H. Clowers, P.E. Haigh, H.H. Hill, Anal. Chem. 75 (2003) 6068.
[26] G.R. Asbury, J. Klasmeier, H.H. Hill Jr., Talanta 50 (2000) 1291.
[27] M. Joshi, Y. Delgado, P. Guerra, H. Lai, J.R. Almirall, Forensic Sci. Int. 188 (2009) 112.
[28] H.H. Hill Jr., Talanta 50 (2000) 1291.
[29] M. Tam, H.H. Hill Jr., Anal. Chem. 76 (2004) 2741.
[30] S.J. Valentine, R.T. Kurulugama, B.C. Bohrer, S.I. Merenbloom, R.A. Sowell, Y. Mechref, D.E. Clemmer, Int. J. Mass Spectrom. 283 (2009) 149.
[31] M.R. Schenauer, J.A. Leary, Int. J. Mass Spectrom. 287 (2009) 70.
[32] P.R. Kemper, N.F. Dupuis, M.T. Bowers, Int. J. Mass Spectrom. 287 (2009) 46.
[33] E.S. Baker, K. Tang, W.F. Danielson, D.C. Prior, R.D. Smith, J. Am. Soc. Mass Spectrom. 19 (2008) 411.
[34] K. Giles, S. Pringle, K. Worthington, R. Bateman, Travelling wave ion propulsion in collision cells, Presented at the 51st American Society of Mass Spectrometry (ASMS) Conference on Mass Spectrometry and Allied Topics, Montreal, Canada, June 2003.
[35] A.A. Schvartsburg, R.D. Smith, Anal. Chem. 80 (2008) 9689.
[36] C.A. Scarff, V.J. Patel, K. Thalassinos, J.H. Scrivens, J. Am. Soc. Mass Spectrom. 20 (2009) 625.
[37] J.P. Williams, T. Bugarcic, A. Habtemariam, K. Giles, I. Campuzano, P.M. Rodger, P.J. Sadler, J. Am. Soc. Mass Spectrom. 20 (2009) 1119.
[38] K. Thalassinos, M. Grabenauer, S.E. Slade, G.R. Hilton, M.T. Bowers, J.H. Scrivens, Anal. Chem. 81 (2009) 248.
[39] Y.T. Chan, X. Li, M. Soler, J.L. Wang, C. Wesdemiotis, G.R. Newkome, J. Am. Chem. Soc. 131 (2009) 16395.
[40] D. Wittmer, Y.H. Chen, B.K. Luckenbill, H.H. Hill Jr., Anal. Chem. 66 (1994) 2348.
[41] Y.H. Chen, H.H. Hill Jr., D.P. Wittmer, Int. J. Mass Spectrom. Ion Process. 154 (1996) 1.
[42] P.W. Cooper, Explosives Engineering, 2nd ed., Wiley, New York, 2008.
[43] R.L. Woodfin, Trace Chemical Sensing of Explosives, Wiley, New York, 2007.
[44] A.C. Shead, Mikrochim. Acta 5 (1967) 936.
[45] J. Almog, A. Klein, A. Sokol, Y. Sasson, D. Sonenfeld, T. Tamiri, Tetrahedron Lett. 47 (2006) 8651.
[46] L.L. Danylewych-May, U.S. Patent 0,192,098, 2006.
[47] G.R. Asbury, H.H. Hill Jr., J. Microcolumn Sep. 12 (2000) 172.
[48] G. Hopfgartner, Part I: Introduction to MS in bioanalysis, in: K.T. Wanner, G. Hofner (Eds.), Mass Spectrometry in Medicinal Chemistry, Wiley-VCH, Weinheim, Germany, 2007, pp. 1–23.
[49] V. Stepanov, L.N. Krasnoperov, I.B. Elkina, X. Zhang, Propell. Explos. Pyrotech. 30 (2005) 178.
[50] R. Tachon, V. Pichon, M.B. Le Borgne, J.J. Minet, J. Chromatogr. A 1154 (2007) 174.
[51] "Ion Mobility Spectrometer–Mass Spectrometer," Product Literature, http://www.excellims.com/pdf/Brochure_03_IMSMS_030709.pdf.
[52] X. Zhao, J. Yinon, Rapid Commun. Mass Spectrom. 15 (2001) 1514.
[53] J.C. Oxley, J.L. Smith, H. Chen, Propell. Explos. Pyrotech. 27 (2002) 209.
[54] W.J. McGann, P. Haigh, J.L. Neves, Int. J. Ion Mobil. Spectrom. 5 (2002) 119.
[55] I. Cotte-Rodriguez, H. Chen, R.G. Cooks, Chem. Commun. (2006) 953.
[56] A.J. Marr, D.M. Groves, Int. J. Ion Mobil. Spectrom. 6 (2003) 59.
[57] G.A. Buttigieg, A.K. Knight, S. Denson, C. Pommier, M.B. Denton, Forensic Sci. Int. 135 (2003) 53.
[58] K. Schug, H.M. McNair, J. Sep. Sci. 25 (2002) 760.
[59] J. Yinon, S. Zitrin, Modern Methods and Applications in Analysis of Explosives, Wiley, New York, 1993.
[60] http://www.globalsecurity.org/military/systems/munitions/explosives.htm.